Chapter 3

Experimental analysis

Experimental validation represents the main issue of this chapter. Another important objective is to deeper analyze the anisotropic effects observed in flows in porous media. In RTM and SRIM processes, a resin is injected into a fiber reinforcement previously placed in a mold. As it will be seen in Chapter 5, this fiber set usually exhibits symmetry properties which can confer anisotropic properties to the matrix. Whereas this topic is frequently considered from a theoretical viewpoint in the literature (8; 26; 33), the experimental viewpoint is seldom addressed. Moreover, there is a serious lack of data in order to validate the developed models. Therefore the aim of the experimental work is threefold. On the one hand, (i) the construction of a porous medium of controlled symmetry is a first challenge, as well as (ii) the conception of the entire experimental device. On the other hand, (iii) deducing medium parameters such as permeability or dispersion tensor components from the measurements and hence validating the models represents another difficult goal.

In this work we have set up a device and a procedure to perform experiments in order to validate Darcy's law. Moreover, this has led us to determine permeability components for specific symmetric media and to confirm some values deduced from theoretical considerations (cf. Chapter 2). However, supplementary experiments should be performed in order to investigate the nonlinear regime in order to highlight for example Forchheimer's effects. Moreover the procedure should be improved in order to completely determine the dispersion tensor. Finally a complementary approach should be developed to study the thermal problem.

The principles and conception of the constructed apparatus are firstly explained and justified. The measurements are then exposed and results are discussed. Finally, conclusions and experimental perspectives are drawn.

This chapter has been mainly inspired from the graduation work of V. Thibaut (3).

3.1 Conception and principles

In this section we describe the conception of the porous medium and of the experimental apparatus. The basic principles governing the experimental procedure are also exposed.

Let us recall that the focus is here on anisotropic porous media. More precisely, so-called transversely isotropic media are especially studied. The anisotropy is therefore "controlled". The transverse isotropy property is conferred to a medium when it exhibits a specific symmetry axis for all rotations around this axis. It is then interesting to compare different relative orientations of the flow with respect to this axis. The experimental apparatus must therefore be constructed in such a way that the medium orientation can be changed relatively to the mean flow direction.

3.1.1 Medium

The conception of the medium has been led by different considerations, viz. (i) that the medium anisotropy must be controlled, (ii) that the relative dimensions of the pores and of the entire medium must be well-chosen and (iii) that the production of several similar media must be easy.

We choose to build the medium by an assembly of small elements resulting in a porous cubic block. Since we are interested by a transversely isotropic medium, the shape of these constitutive elements must be the same after any rotation around their symmetry axis. Obviously the statistical averaging process must be taken into account to reach the desired symmetry and the orientation of the individual elements can vary in a random way. "Needles" and "discs" answer this objective. For practical reasons, only the medium consisting of needles has been selected for our tests.

In order to build a representative macroscopic medium, the length of the "needles" must be at least one order of magnitude smaller than the entire block. Fibers of 1 mm diameter and 15 mm length and an entire 10 cm $\times$ 10 cm $\times$ 10 cm medium seem to be a pertinent compromise. With these dimensions and shape, one block indeed contains about 50000 to 60000 needle elements and the porous block is easy to design and construct.

Finally, in order to facilitate the medium assembly process, polymeric needles were selected. Indeed, with this matter, the formation of a coherent medium is automatically carried out by heating and reticulation. Of course care must be given to almost identically orienting the needles in the mold before starting the reticulation in the drying oven.

3.1.2 Apparatus

To produce a flow through a porous medium, the underlying principle consists in imposing a pressure gradient. In our experiment, this gradient is induced by a liquid height difference between the entry and the exit. In the conception of our apparatus, the medium is then inserted in a given orientation into a column containing the fluid, while taking care of watertightness near the borders. Moreover, as we are interested in flows in saturated porous media, the exit level is roughly situated at the same height as the middle of the medium and a siphon is introduced (Fig. 3.1).

In order to determine the permeability and dispersion coefficients, specific features are set up and the the measuring device is adapted to each case.

A runoff system is built in order to maintain a constant pressure on the top side of the porous medium. The pressure on the other side is controlled by the height of a barrier in the collector. The latter is designed in such a way that the fluid velocity be low. The flow rate measurement can then be sufficiently accurate.

In order to quantify the mixing effect of the porous medium, the device has been further adapted. First of all, in order to enable the flow of two distinct by coloured fluids, watertight separations were introduced on the top side of the block (Fig. 3.2). Mixed fluids are then collected at the bottom of the block in twelve separated zones. A siphon system is still used in order to avoid void formation.

The complete experimental set-up can be found in (3) together with the measurement details.

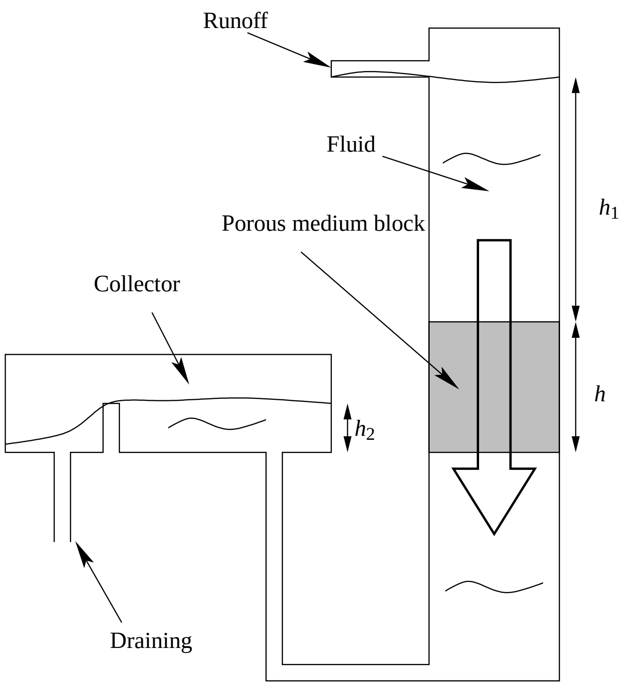

Figure 3.1: Experimental scheme - Flow rate resulting from an imposed pressure difference.

3.2 Measurements and results

In this section, we expose the principles we have followed in order to measure the permeability and dispersion components from the measurements. Experimental measurements are detailed and the deduced medium properties are discussed.

3.2.1 Permeability

Since experiments described in Fig. 3.1 deal with a 1D mean flow, we can rewrite the 1D Darcy equation in macroscopic terms as :

$$V = -\frac{K}{\eta}\frac{\Delta P}{h} \tag{3.2.1}$$

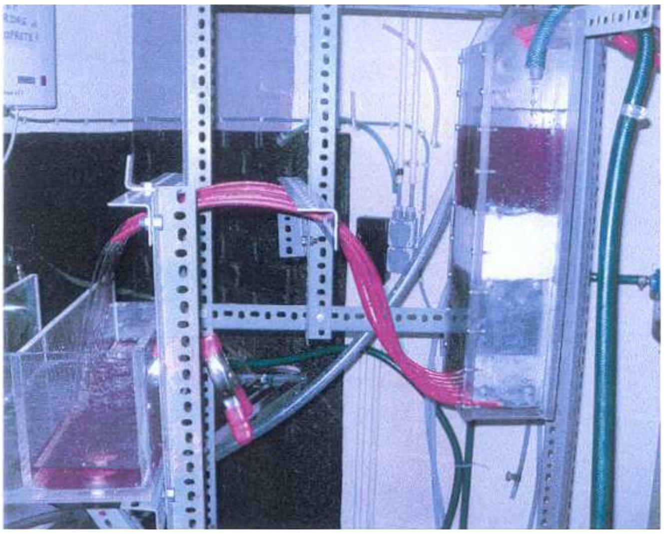

(a)

(b)

Figure 3.2: (a) Siphon system in order to avoid void formation and to maintain a constant exit pressure. (b) Separated zones at the entry and the exit of the porous medium.

where V is the macroscopic fluid velocity, η the fluid viscosity, ΔP the pressure difference along the medium depth (h) and K the permeability in the flow direction. Since our experiments measure flow rates, we rewritte Eq. (3.2.1) as :

$$Q = -\frac{K}{\eta}\frac{\Delta P}{h}S, \tag{3.2.2}$$

where Q denotes the flow rate across the medium section S. Knowing the dimensions of the block, the fluid viscosity, the pressure drop, and the measured flow rates, the permeability component in the mean flow direction can be written as :

$$K = -\frac{Q\eta}{\Delta P}\frac{h}{S}\ . \tag{3.2.3}$$

In Chapter 5, it will be proved that the permeability tensor for a transversely isotropic medium is determined by two parameters only, one for the permeability along the symmetry axis and the second for the permeability along any perpendicular direction. These components are denoted by $K_{\|}$ and $K_{\perp}$ respectively. Considering our previous comments, these two components can be determined by aligning the needle direction parallel or perpendicular to the mean flow direction.

The experiments were repeated several times on two macroscopically similar porous blocks in order to assess the validity of the measurements, and the entire procedure was repeated twice (noted Exp1 and Exp2) to verify its pertinence. In order to determine the flow rate, the time for a fixed fluid volume to run across the porous block was measured. Table 3.1 summarizes the detailed measurements for all handlings (Table C.1).

Table 3.1: Mean time [s] taken by one water liter to flow across the porous medium

	Medium 1		Medium 2	
	$\|$ case	$\perp$ case	$\|$ case	$\perp$ case
Exp 1	29.2284	33.5436	28.0563	32.2741
Exp 2	29.7313	33.7776	27.5484	32.3534
Mean Time	29.4799	33.6606	27.8024	32.3138

Let us first observe that both classes of measurements are consistant. This seems to validate the measurement procedure. Moreover, the running time is clearly higher in the perpendicular case than in the parallel case. As it appears intuitively, this indicates that the perpendicular permeability component ($K_{\perp}$) is larger than the parallel component ($K\,\|$). This assertion is confirmed by results of Table 3.2 where we observe that

Table 3.2: Permeability components from the measurements

	Medium 1		Medium 2	
	$\parallel$ case	$\perp$ case	$\parallel$ case	$\perp$ case
Viscosity η [Pa.s]	$1.12\ 10^{-3}$	$1.14\ 10^{-3}$	$1.14\ 10^{-3}$	$1.14\ 10^{-3}$
Flow rate Q [m^{3}s^{-1}]	$3.4\ 10^{-5}$	$2.97\ 10^{-5}$	$3.6\ 10^{-5}$	$3.09\ 10^{-5}$
Pressure difference ΔP [Pa]	$1.2753\ 10^{3}$	$1.2753\ 10^{3}$	$1.2753\ 10^{3}$	$1.2753\ 10^{3}$
Deduced permeability K [m^2]	$2.96\ 10^{-10}$	$2.65\ 10^{-10}$	$3.21\ 10^{-10}$	$2.76\ 10^{-10}$

the parallel component is from 13% to 14% higher than the perpendicular one. Even if this difference is low, it is the same in both cases.

In order to validate the Darcy law, this experiment should have been repeated for different pressure drops. Nevertheless, it must be noted that our experimental flows lie well in the linear regime. Indeed, the **pore sized Reynolds number** is much smaller than unity :

$$Re_p = \frac{\rho V \sqrt{K}}{\eta} \approx 0.05 < 1. \tag{3.2.4}$$

3.2.2 Dispersion

In order to analyse the mixing effect induced by dispersion, two equivalent but distinguishable fluids are injected at the medium entry. The distinction is obtained by the adjunction of potassium permanganate in one of the entering fluids (Fig. 3.2) and the observations are based on measuring the concentration of this substance at the exit of the porous block. Two cases are again studied, with the mean flow perpendicular or parallel to the needle direction, respectively (Fig. 3.3 (a) and (b)). It should however be noted that another case could be considered in the 'perpendicular' case, viz. when the porous medium is oriented in such a way that the needles are perpendicular to the flow, but parallel to the impermeable wall separating the two different coloured fluids.

In a first step, we focus on the perpendicular case (a) and examine the equation governing the concentration evolution. Choosing the x-axis as aligned with the symmetry axis of the medium, the macroscopic equation for concentration Eq. (1.7.103) roughly

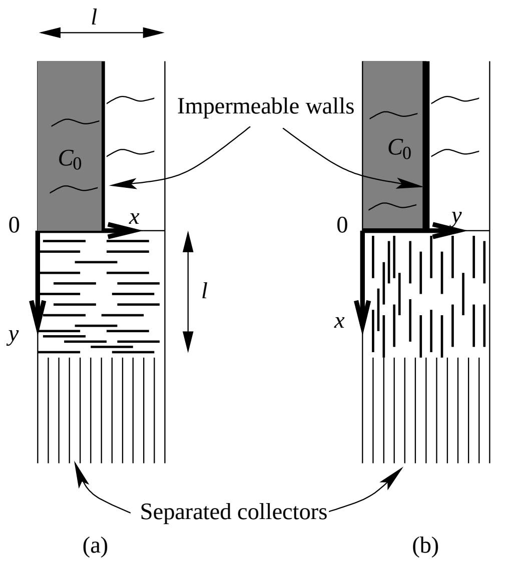

Figure 3.3: Experiment scheme and boundary conditions for the determination of dispersion. (a) Flow perpendicular to the needle direction ; (b) Flow aligned with the needle direction.

simplifies in the stationary case and without any source term as :

$$V\frac{\partial C}{\partial y} = D_{x,y}\frac{\partial^2 C}{\partial x^2} + D_{y,y}\frac{\partial^2 C}{\partial y^2}, \tag{3.2.5}$$

where $D_{x,y}$ and $D_{y,y}$ denote the total diffusion components (molecular diffusion + dispersion effect) and V is the macroscopic velocity as aligned with the y-axis. Moreover the total diffusion tensor can here be assumed being diagonal.

The boundary conditions are :

$$\begin{cases} C = C_0, & 0 \le x < l/2 \quad y = 0, \\ C = 0, & l/2 \le x < l \quad y = 0, \end{cases} \quad \text{and} \quad \begin{cases} \frac{\partial C}{\partial x} = 0, & x = 0 \\ \frac{\partial C}{\partial x} = 0, & x = l\ . \end{cases} \tag{3.2.6}$$

Considering the boundary conditions and mean flow path, **we will in addition assume that in what follows diffusion in the flow direction is negligible in front of convection and of diffusion in the perpendicular direction**. This is a quite strong hypothesis. In this first attempt, Eq. (3.2.5) can be rewritten as :

$$V\frac{\partial C}{\partial y} = D_{x,y}\frac{\partial^2 C}{\partial x^2}\ . \tag{3.2.7}$$

The solution of this equation is easily obtained by variable separation and is equal to :

$$\frac{C}{C_0} = \frac{1}{2} + \sum_{k=0}^{\infty} \frac{(-1)^k}{(2k+1)\frac{\pi}{2}} \exp\left(-\left(\frac{(2k+1)\pi}{l}\right)^2 \frac{y\, D_{x,y}}{V}\right) \cos\left(\frac{(2k+1)\pi}{l}\, x\right) . \tag{3.2.8}$$

Finally, $D_{x,y}$ is deduced by fitting this solution with the measurements.

In order to measure the concentrations, the spectrometry technology was used. At the entry, a given side of the column was filled with pure water while the other side was filled with water colored by means of permanganate with a starting concentration of 99.5 ppm. Samples of colored liquid were then collected in separated zones at the porous block exit when steady-state flow regime was reached. The concentration of each sample was then measured while noting its position in the exit zone. Hence, graphs of concentration distribution were finally drawn. This procedure was again repeated several times for both blocks in order to validate the measurements (Fig. 3.4). Since the results are very close together for both blocks (Figs. 3.4 and 3.5), this tends to validate the experimental procedure.

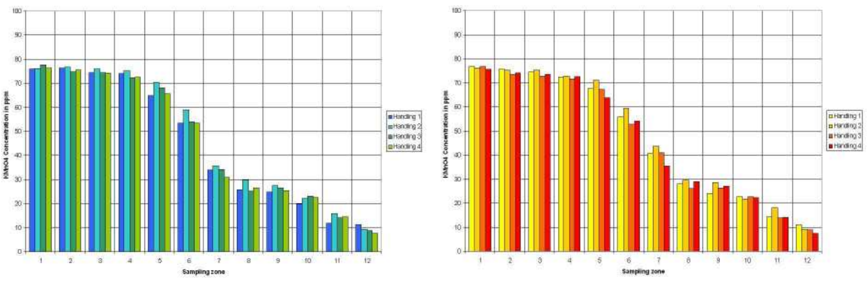

Figure 3.4: Concentration distribution at the exit of the porous block in twelve separated zones (3). The flow is perpendicular to the medium symmetry axis (Fig. 3.3 (a)). The experiments were performed with the first and with the second block (left and right figures).

Fitting the solution (3.2.8) with the experiments finally gives the coefficient $D_{x,y}$ for both blocks :

$$D_{x,y} = 1.984\ 10^{-5}\ \mathrm{m^2 s^{-1}} \quad \text{and} \quad D_{x,y} = 2.076\ 10^{-5}\ \mathrm{m^2 s^{-1}}. \tag{3.2.9}$$

A similar approach has been applied in order to determine $D_{y,x}$ in the parallel case. In that case again, **the diffusion in the flow direction was assumed to be negligible**

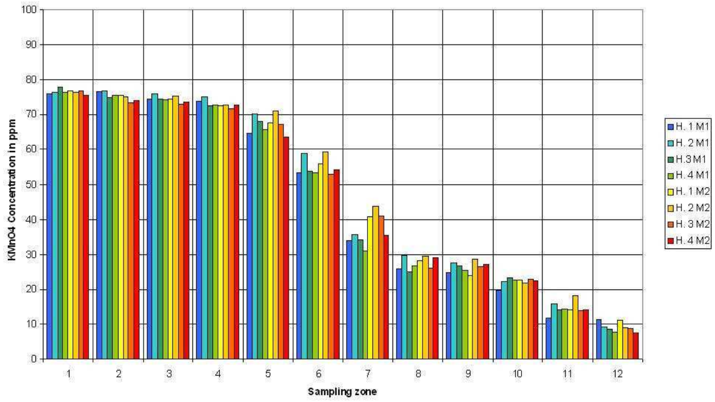

Figure 3.5: Flow perpendicular to the medium symmetry axis (Fig. 3.3 (a)). Similar results are obtained for the concentration distribution in both media (3).

in front of convection and perpendicular diffusion. The related measurements are again consistant for both blocks (Fig. 3.6) and the fitting of the experimental results with the simplified equation solution gives :

$$D_{y,x} = 6.095\ 10^{-6}\ \mathrm{m^2 s^{-1}} \quad \text{and} \quad D_{y,x} = 6.864\ 10^{-6}\ \mathrm{m^2 s^{-1}}. \tag{3.2.10}$$

Analyzing the experimental results (Figs. 3.4 and 3.6) shows that the perpendicular case induces more mixing than the parallel case. The diffusion components determined in Eqs. (3.2.9) and (3.2.10) confirm these observations. However, it should be recalled that these results are based on the assumption of neglecting diffusion in the flow direction.

A more accurate approach should consist in working without this assumption and in determining the total diffusion components by comparing additional results with measurements. However, the calculation becomes more complicated and further developments are needed.

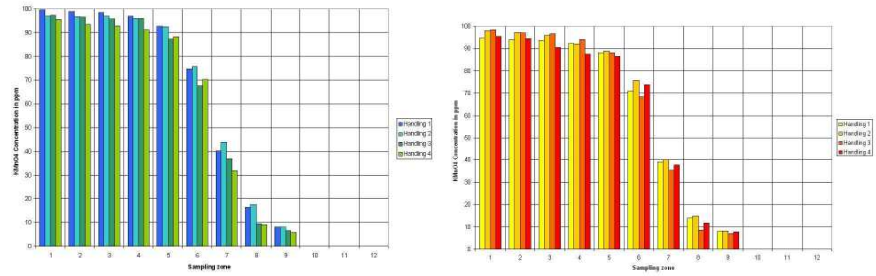

Figure 3.6: Concentration distribution at the exit of the porous block in twelve separated zones (3). The flow is parallel to the medium symmetry axis (Fig. 3.3 (b)). The experiments were performed with the first and with the second block (left and right figures).

3.3 Conclusions

The experiments described in this chapter have enabled us to build an experimental set-up and to draw a procedure in order to capture some effects specific to flows in porous media. There is a serious lack of references in this domain, and this work can be seen as a first step in the difficult experimental analysis and validation of the theory of mechanical dispersion.

In further work, the permeability experiment should be repeated for different pressure drops in order to validate Darcy's law. The tensorial form of permeability should also be verified by performing experiments with the "needle" direction oriented at different angles with respect to the mean flow direction. Nonlinear laws (such as Forchheimer's law) should finally be investigated at high flow rates, and the related coefficient should be measured.

It should here be noted that, in all the experiments, we have implicitly assumed that the capillary forces are negligible. Certainly this is the case for our experiment since the needles are assumed to be completely wetted.

Concerning mechanical dispersion, the experimental procedure should be refined in order to determine all the dispersion components. The assumption of negligible diffusion in the flow direction should also be verified or a more accurate measurement technique should be used. In Chapter 5, it will be seen that only six parameters are sufficient to determine the dispersion tensor for a transversely isotropic medium.

Supplementary experiments should then be carried out in order to determine all of these dispersion components. Typically, if the other 'perpendicular' case could have been considered, the component $L_{\perp\perp}$ could have then been determined. Finally, non-stationary experiments should be performed and various boundary conditions should be implemented.

At the present stage, assuming that molecular diffusion is negligible in front of hydrodynamic dispersion, we have been able to determine some parameters of the dispersion tensor. Indeed in this case, the fitting of $D_{x,y}$ and $D_{y,x}$ to the dispersion model (5.2.35) for a transversely isotropic medium gives :

$$L_{\parallel\perp} = 6.5 10^{-3}\text{m} \quad \text{and} \quad L_{\perp\parallel} = 2.15 10^{-3}\text{m}. \tag{3.3.11}$$

The unique values we have found in the literature are given by Mal et al. in (26), who use coefficients two orders of magnitude lower than these values. Obviously, the considered medium was different in their experiments.

In Chapter 2, numerical experiments were performed with the parameters fitted on the present needle-made medium. In these numerical experiments, boundary conditions were imposed in such a way that the parallel permeability component was playing the major role. A value of $3.5\ 10^{-10}\ \text{m}^2$ was found. This value is very similar to the experimental result of this chapter (Table 3.2). However, the fitting required to determine the parameters of the micro-macro model is not obvious and is probably not unique. Hence, concluding that our model and experiments perfectly agree is too hasty but instead leads to more investigations. Similar calculations for the perpendicular component further give $K_{\perp} = 6.7 10^{-11}\ \text{m}^2$, which is by far smaller than the experimental value.

The thermal problem has not been tackled in this chapter. It requires more experimental tools and a more expensive apparatus. This was not mandatory at the present research stage and we did not investigate this issue.

Finally, let us recall that the main goals of this chapter were (i) to demonstrate the possibility of implementing experiments on media with controlled anisotropy, (ii) to validate the governing laws for permeability and dispersion in such media, and finally (iii) to deduce the medium material parameters from the measurements. Whereas the analysis is not complete at this stage, it indicates that our method is appropriate for these goals.